




# Multicomponent altermagnet: A general approach to generating multicomponent structures with two-dimensional altermagnetism

Hongjie Peng, Sike Zeng , Ji-Hai Liao, Chang-Chun He , \* Xiao-Bao Yang, and Yu-Jun Zhao 

*Department of Physics, South China University of Technology, Guangzhou 510640, China*



(Received 23 February 2025; revised 21 April 2025; accepted 28 April 2025; published 13 May 2025)

Altermagnetism, as an unconventional antiferromagnetism, exhibits collinear-compensated magnetic order in real space and spin-splitting band structure in reciprocal space. In this work, we propose a general approach to generating multicomponent structures with two-dimensional (2D) altermagnetism, based on symmetry analysis. Specifically, by analyzing the space group of the crystal structures and their subgroups, we systematically categorize equivalent atomic positions and arrange them into orbits based on symmetry operations. Chemical elements are then allowed to occupy all atomic positions on these orbits, generating candidate structures with specific symmetries. We present a general technique for generating collinear-compensated magnetic order, characterized by the symmetrical interconnection between opposite-spin sublattices, and employ first-principles calculations to determine magnetic ground states of multicomponent materials. This approach integrates symmetry analysis with the screening of altermagnetic configurations to evaluate the likelihood of candidates possessing altermagnetism. To verify the methodology, we provide examples of previously unreported 2D altermagnets, such as  $\text{Cr}_2\text{Si}_2\text{S}_3\text{Se}_3$ ,  $\text{Fe}_2\text{P}_2\text{S}_3\text{Se}_3$ , and  $\text{V}_2\text{O}_2\text{BrI}_3$ , and evaluate their dynamical stability by calculating the phonon spectrum. The results demonstrate the feasibility of our approach in generating stable multicomponent structures with two-dimensional altermagnetism. Our research has significantly enriched the candidate materials for 2D altermagnets, and provides a reference for experimental synthesis.

DOI: [10.1103/PhysRevB.111.195123](https://doi.org/10.1103/PhysRevB.111.195123)

## I. INTRODUCTION

Magnetic moments interact in intricate ways, producing diverse magnetic phases, including conventional ferromagnetism, antiferromagnetism, as well as altermagnetism, which has recently attracted significant attention in condensed matter physics [1–12]. Altermagnetism, as an unconventional antiferromagnetism, exhibits collinear-compensated magnetic order in real space, but it is characterized by broken time-reversal symmetry leading to spin splitting in reciprocal space. Conventional antiferromagnets exhibit spin degeneracy in the band structure because the opposite-spin sublattices are connected through inversion or translation symmetry [3]. However, in altermagnets, the opposite-spin sublattices are interconnected through crystal symmetry operations (such as rotation, mirror, and glide reflection) rather than through inversion or translation symmetries, leading to the disruption of  $PT$  symmetry [3]. Recent experimental breakthroughs utilizing angle-resolved photoemission spectroscopy have successfully identified spin-splitting electronic structures in altermagnets, providing direct evidence for the existence of altermagnetism [13–17].

Compared to the numerous three-dimensional altermagnets that have been discovered, two-dimensional intrinsic altermagnets are rarely reported [4]. Unlike three-dimensional collinear magnetic materials, the connection between opposite-spin sublattices through  $m_z$  (the mirror op-

eration in the  $xy$  plane) or  $C_{2z}$  (twofold rotation around the  $z$  axis) protects the spin degeneracy of the nonrelativistic band structure for all  $\mathbf{k}$  vectors in the whole Brillouin zone in two-dimensional collinear magnetic materials [18]. This is one contributing factor to the rarity of discovered two-dimensional altermagnets. Therefore, a series of methods for searching for or generating two-dimensional altermagnets have been proposed [19–21], for instance, high-throughput computational screening [19]. Although high-throughput computational screening has been employed, the resultant number of two-dimensional altermagnets remains relatively limited, primarily due to the fact that the majority of two-dimensional magnetic materials possessing collinear magnetic configurations do not fulfill the symmetry prerequisites for altermagnets. Moreover, transition from conventional antiferromagnetism to altermagnetism in two-dimensional magnetic materials can be induced by application of an external electric field [20]. Application of an out-of-plane electric field to  $\text{MnPS}_3$  or  $\text{MnPSe}_3$  can also break the  $PT$  symmetry and induce extrinsic two-dimensional altermagnetism. In addition, bilayer stacking is a successful general approach to generating two-dimensional altermagnetism [21,22]. Constructing a bilayer system comprising two single ferromagnetic layers with antiferromagnetic coupling can induce altermagnetism. In this way, the bilayer system satisfies the requirement that the opposite sublattices can be connected by symmetries, but  $C_{2z}$  and  $z$ -direction translation symmetry between the opposite-spin sublattices are excluded, making it easier for the bilayer system to possess altermagnetism.

\*Contact author: scuthecc@scut.edu.cn

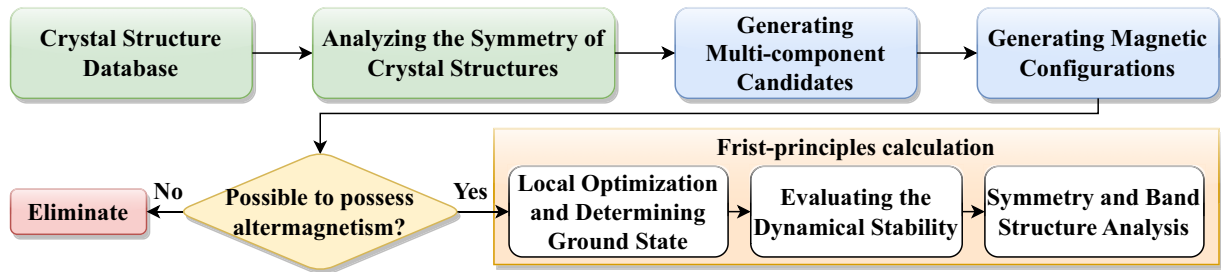


FIG. 1. Framework for generating stable multicomponent altermagnets. We propose a general approach to generating multicomponent 2D altermagnetic structures and magnetic configurations based on symmetry analysis of crystal structures. The method combines symmetry analysis with screening of altermagnetic configurations, followed by first-principles calculations to determine magnetic ground states and dynamical stability. Symmetry and band structure analysis confirm altermagnetism in candidate structures.

The expansion of two-dimensional materials with altermagnetism will greatly enhance our understanding of the fundamental properties of altermagnets and promote their applications in spintronics; for instance, giant and tunneling magnetoresistance (GMR and TMR) effects [16] can be generated in altermagnets. Therefore, developing an approach to enriching two-dimensional altermagnetic structures is of great significance. Moreover, given the absence of experimentally synthesized two-dimensional (2D) altermagnets, it is crucial to establish a reliable method for predicting stable 2D altermagnets.

In this work, we propose a general approach to generating multicomponent structures that possibly exhibit two-dimensional altermagnetism, based on group-subgroup relationship and symmetry analysis of crystal structures sourced from the Computational 2D Materials Database (C2DB) [23,24]. Furthermore, we also propose a general method for generating collinear magnetic configurations characterized by the symmetric interconnection of opposite-spin sublattices. This approach merges symmetry analysis with the screening of altermagnetic configurations to ascertain the potential of candidate structures to possess altermagnetism. Employing first-principles calculations, we conduct local optimization and determine magnetic ground state of these candidates. Following this, we identify structures with dynamical stability by computing of their phonon spectrum. Finally, we conduct a thorough analysis of symmetry and band structure to demonstrate that the candidate structures possess altermagnetism. In conclusion, our work presents a general methodology for generating stable multicomponent structures exhibiting two-dimensional altermagnetism, as shown in Fig. 1. This contributes to the diversification of 2D altermagnets and offers a reference for the experimental synthesis.

In our previous study, we demonstrated that structures with a small number of Wyckoff positions exhibit a high likelihood of being ground state structures of multicomponent materials [25]. This method is capable of generating candidate structures with specific symmetries and a small number of Wyckoff positions. Therefore, this approach to generating symmetric structures is also beneficial for identifying stable configurations of multicomponent materials.

The article is organized as follows: in Sec. II, we present a general approach to generating multicomponent structures with altermagnetism. In Sec. III, we introduce a method

for generating collinear magnetic configurations with features of the connection between opposing sublattices through symmetries. In Sec. IV, we present examples of previously unreported 2D multicomponent altermagnets to validate our approach and analyze their dynamical stability. Finally, we summarize our findings for 2D altermagnetism.

## II. AN APPROACH TO GENERATING A MULTICOMPONENT ALTERMAGNET

We propose a method for generating multicomponent structures possessing specific symmetry, as shown in Fig. 2. To construct multicomponent altermagnets, which require particular symmetry, it is essential to ensure that the candidate structures exhibit specific symmetry. Altermagnetic materials demand that the opposite sublattices occupied by opposite spins are connected by symmetry operations, such as rotation or mirror operations [3], which are among symmetry operations possessed by the crystal structure. Hence, candidates possessing the required symmetry are indispensable for exhibiting altermagnetism. Utilizing the method introduced in this section, we generate a series of candidates fulfilling these symmetry conditions. Initially, we analyze the space (layer) group of a materials class sharing the same symmetry and group-subgroup relationships. Based on the primitive cell or supercell, we assign the equivalent atomic positions into different orbits according to the subgroup. By populating these orbits with elements, we generate a series of candidates with specific symmetries.

The symmetry of crystal structures aligns with a specific space (layer) group, denoted as  $G$ . Based on the primitive cell or supercell, we analyze all subgroups of the group  $G$  and organize them into subgroup chains. Let  $X$  be a nonempty set that includes all equivalent atomic positions in the structure,  $X = \{x_1, x_2, x_3, \dots, x_i, \dots\}$ . Let  $G$  be the transformation group on  $X$ . If for all  $x_i, x_j \in X$  there exists  $g \in G$  such that  $g(x_i) = x_j$ , meaning there is a crystallographic symmetry operation in  $G$  that relates the positions  $x_i$  and  $x_j$ , then  $x_i$  and  $x_j$  are regarded to be equivalent. The set of all positions in  $X$  that are equivalent to the positions  $x_i$ , which is the collection of all positions that can be mapped to  $x_i$  through the symmetry operations of the group  $G$ , is referred to as the  $G$  orbit of  $x_i$ . When selecting a subgroup  $H_k$  from the subgroup chain, divide each class of equivalent atomic positions with subgroup  $H_k$  into different orbits. The  $H_k$  orbit of

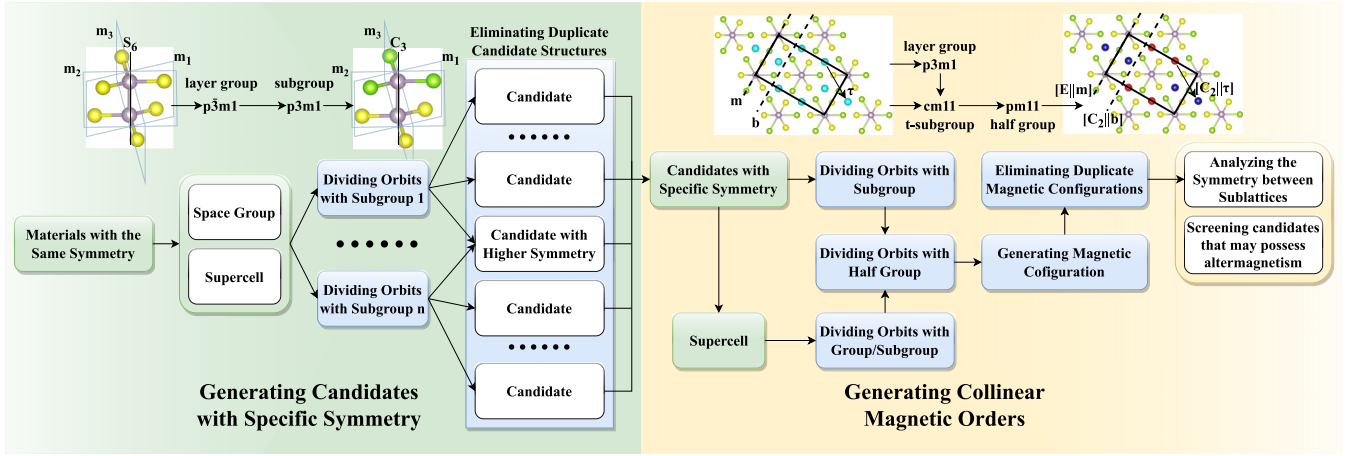


FIG. 2. An approach to generating multicomponent candidates that exhibit particular symmetry requirements of altermagnetism and collinear magnetic orders with features of the connection between opposing sublattices through symmetries. The figure consists of two parts: the left side depicts the approach to generating candidate structures, introduced by Sec. II, while the right side depicts the approach to generating collinear magnetic configurations, introduced by Sec. III.

general position  $x$  is  $\{x, h_1x, h_2x, \dots, h_nx\} = \{hx \mid h \in H_k\}$ . This process involves categorizing the equivalent atomic positions based on the symmetry operations represented by the subgroup  $H_k$ . The orbits are essentially the sets of points that can be mapped onto each other through the symmetry operations of the subgroup  $H_k$ . After obtaining the orbits, we populate these orbits with elements and generate a series of candidates  $\{S_1, S_2, \dots, S_j, \dots\}$  that satisfy the symmetry requirements of  $H_k$ .

We provide a simple proof to demonstrate that the candidate structures  $\{S_1, S_2, \dots, S_j, \dots\}$  satisfy the symmetry requirements of group  $H_k$ . Let the position of the  $i$ th atom in the  $m$ th component of the candidate structure  $S_j$  be denoted as  $\vec{r}_i^{(m)}$ . Define the set  $R_m = \{\vec{r}_1^{(m)}, \vec{r}_2^{(m)}, \dots, \vec{r}_i^{(m)}, \dots, \vec{r}_n^{(m)}\}$ , where  $n$  is the number of atoms contained in the  $m$ th component. According to the definition of the subgroup  $H_k$  orbit, for all  $\vec{r}_i^{(m)} \in R_m$  and  $h_\alpha \in H_k$ , there exists  $\vec{r}_j^{(m)} \in R_m$  such that  $\vec{r}_i^{(m)} = h_\alpha \vec{r}_j^{(m)}$ , which means  $H_k$  keeps  $R_m$  invariant. Each component has  $R_m = h_\alpha R_m$ , where  $h_\alpha \in H_k$ , which means the subgroup  $H_k$  of group  $G$  keeps the candidate structure  $S_j$  unchanged. When identical components occupy distinct subgroup orbits, they may enable the candidate structure  $S_j$  to meet higher symmetry requirements, without impairing the ability of the subgroup  $H_k$  of group  $G$  to keep the candidate structure  $S_j$  unchanged. For instance, identical components occupying different orbits  $\{hx \mid h \in H_k\}$  and orbits transformed by  $g_\alpha$  as  $g_\alpha\{hx \mid h \in H_k\}$  (where  $g_\alpha$  belongs to the set  $G - H_k$ , meaning  $g_\alpha$  is an element of  $G$  but not of  $H_k$ ) result in an additional symmetry operation  $g_\alpha$ , which keeps the candidate structure  $S_j$  unchanged. Therefore, the symmetry of the candidate structures  $\{S_1, S_2, \dots, S_j, \dots\}$  corresponds to at least the subgroup  $H_k$ .

Iterating through all possible ways of components occupying orbits will lead to equivalent candidate structures. Equivalent candidate structures result in redundant analysis and first-principles calculations, so it is necessary to eliminate equivalent structures. Both structures generated by different subgroups and those by the same subgroup may exhibit rep-

etition. If two candidate structures can be connected by a symmetry  $g_\alpha$  (where  $g_\alpha \in G$ ), then they are equivalent. Let  $S$  be a nonempty set that includes all candidate structures,  $S = \{S_1, S_2, \dots, S_j, \dots\}$ , where the elements  $S_1, S_2, S_3, \dots$  are the candidate structures. Group  $G$  is the transformation group on  $S$ . Since the subgroup  $H_k$  of group  $G$  keeps the candidate structure  $S_j$  unchanged,  $H_k = \{h \mid h \in G \text{ and } hS_j = S_j\}$ . Then  $H_k$  is the isotropy subgroup of  $G$  for the candidate structure  $S_j$ . Therefore, the equivalent structures on the  $G$  orbit of the candidate structure  $S_j$ ,  $\{S_j, g_1S_j, g_2S_j, \dots, g_nS_j\}$ , correspond one to one with the left cosets of  $H_k$ . In this way, we identify and eliminate a portion of the equivalent candidate structures.

### III. AN APPROACH TO GENERATING COLLINEAR MAGNETIC CONFIGURATIONS

After obtaining the atomic arrangement of the magnetic candidate structures, it is necessary to determine the magnetic ground states. To do this, all possible magnetic configurations of the candidate structures must be generated, and then first-principles calculations are used to determine the energy and identify the magnetic ground state. Antiferromagnetic configurations require that the opposite-spin sublattices can be connected by symmetry operations. Therefore, we generate a series of collinear magnetic configurations whose sublattices can be connected by symmetry operations. Based on the symmetry operations that connect opposite sublattices of the altermagnetic configurations in real space, we determine whether the magnetic configurations are possible to possess altermagnetism. If there are configurations with altermagnetism among the collinear magnetic configurations, then it is considered that the candidates are possible to possess altermagnetism. We retain those candidates which have altermagnetic configurations. Then, we use first-principles calculations to determine the energy and find the magnetic ground states of different candidates. In the end, we identify candidates whose ground state is altermagnetic.

We propose a general method for generating collinear magnetic configurations with features of the connection

between opposing sublattices through symmetry operations, and combine it with a method for screening altermagnetic configurations to address whether the candidates possess altermagnetism. The symmetry of the structure corresponds to the space (layer) group  $G$ , and the set of generators of group  $G$  is  $\langle f_1, f_2, \dots, f_m \rangle$ . Each individual generator  $f_i$  in  $\langle f_1, f_2, \dots, f_m \rangle$  can generate a cyclic group of order  $n_i$ , and  $f_i$  cannot be expressed by  $\{f_j \mid j \neq i\}$ . The set of generators  $\langle f_1, f_2, \dots, f_{i-1}, f_{i+1}, \dots, f_m \rangle$  can produce a group  $H$ . Since  $f_i$  cannot be expressed by  $\{f_j \mid j \neq i\}$ ,  $H$  does not contain  $f_i, f_i^2, \dots, f_i^{n_i-1}$ , so it is a subgroup of  $G$ . According to the coset theorem,  $f_i H, f_i^2 H, \dots, f_i^{n_i-1} H$  are obviously disjoint from  $H$  and have no common elements. Therefore, the group  $G$  can be decomposed into a coset string of subgroup  $H$ ,  $G = \{f_i, f_i^2, \dots, f_i^{n_i} = E\} \otimes_S H$ . The notation  $\otimes_S$  denotes the semidirect product. Let  $x$  be a position occupied by a magnetic atom,  $H_x = \{hx \mid h \in H\}$  is the  $H$  orbit of  $x$ , and  $G_x = \{gx \mid g \in G\}$  is the  $G$  orbit of  $x$ . Clearly,  $H_x \subseteq G_x$ . Because the coset strings  $f_i H, f_i^2 H, \dots, f_i^{n_i} H = H$  have no common elements and the same number of elements, the sets  $\{gx \mid g \in f_i H\}, \{gx \mid g \in f_i^2 H\}, \dots, \{gx \mid g \in f_i^{n_i} H\}$  also have no common elements and the same number of elements when  $x$  is a general position. Since  $G = f_i H \cup f_i^2 H \cup \dots \cup f_i^{n_i} H$ , it follows that

$$\begin{aligned} G_x &= \{gx \mid g \in G\} = \{gx \mid g \in (f_i H \cup f_i^2 H \cup \dots \cup f_i^{n_i} H)\} \\ &= \{gx \mid g \in f_i H\} \cup \{gx \mid g \in f_i^2 H\} \\ &\quad \times \cup \dots \cup \{gx \mid g \in f_i^{n_i} H\}. \end{aligned}$$

For generating collinear magnetic configurations, we focus on the case where  $n_i$  is even. When  $n_i = 2$ , the group  $G$  is decomposed into coset strings  $H, f_i H$ . When  $n_i$  is even and  $n_i > 2$ , the generators  $\langle f_i^2, f_1, f_2, \dots, f_m \rangle$  (excluding  $f_i$ ) can produce a subgroup  $H$ . Clearly, the subgroup  $H$  does not contain the group element  $f_i$ . Following this, group  $G$  is decomposed into coset strings  $H, f_i H$ . Therefore, it follows that  $G_x = \{gx \mid g \in G\} = \{hx \mid h \in H\} \cup \{gx \mid g \in f_i H\} = \{hx \mid h \in H\} \cup f_i \{hx \mid h \in H\} = H_x \cup f_i H_x$ , when  $x$  is a general position. When  $n_i$  is even,  $f_i$  decomposes the  $G$  orbit  $G_x$  of a general position  $x$  into two equal parts with a same number of elements  $H_x$  and  $f_i H_x$ . The subgroup  $H$  is referred to as a half group of the group  $G$ .  $H_x$  and  $f_i H_x$  are referred to as half orbits. When magnetic atoms occupy  $l$  nonequivalent positions, the group  $G$  divides the positions of these magnetic atoms into  $l$  distinct orbits, each of which corresponds to  $l$  pairs of half orbits. From each pair of half orbits, one is chosen to form the set  $O_{|\uparrow\rangle}$ , where each atomic position  $x$  is occupied by an up spin; union of the remaining coset orbits form the set  $O_{|\downarrow\rangle}$ , where each atomic position  $x$  is occupied by a down spin. There are  $2^l$  ways to do this.  $O_{|\uparrow\rangle}$  and  $O_{|\downarrow\rangle}$  describe the opposite sublattices and magnetic configurations of the structure. This method generates magnetic configurations  $\{M_1, M_2, \dots, M_j, \dots\}$ .

The union of coset orbits occupied by up spins is

$$O_{|\uparrow\rangle} = \{hx_1 \mid h \in H\} \cup \{hx_2 \mid h \in H\} \cup \dots \cup \{hx_l \mid h \in H\}.$$

The union of coset orbits occupied by down spins is

$$\begin{aligned} O_{|\downarrow\rangle} &= \{gx_1 \mid g \in f_i H\} \cup \{gx_2 \mid g \in f_i H\} \cup \dots \cup \\ &\quad \times \{gx_l \mid g \in f_i H\}. \end{aligned}$$

Therefore,

$$\begin{aligned} f_i O_{|\uparrow\rangle} &= f_i(\{hx_1 \mid h \in H\} \cup \{hx_2 \mid h \in H\} \cup \dots \cup \\ &\quad \times \{hx_l \mid h \in H\}) \\ &= (f_i\{hx_1 \mid h \in H\}) \cup (f_i\{hx_2 \mid h \in H\}) \cup \dots \cup \\ &\quad \times (f_i\{hx_l \mid h \in H\}) \\ &= \{gx_1 \mid g \in f_i H\} \cup \{gx_2 \mid g \in f_i H\} \cup \dots \cup \\ &\quad \times \{gx_l \mid g \in f_i H\} \\ &= O_{|\downarrow\rangle}. \end{aligned}$$

This indicates that  $O_{|\uparrow\rangle}$  and  $O_{|\downarrow\rangle}$  can be connected through the symmetry operation  $f_i$ . When magnetic configuration  $M'_j$  can be obtained from  $M_j$  by spin reversal, these two magnetic configurations are equivalent. Thus, out of the total of  $2^l$  ways to choose, there are at most  $2^{l-1}$  inequivalent choices. In addition to the symmetry operation  $f_i$ , there may be other symmetry operations  $g_\alpha$  (where  $g_\alpha \in f_i H$ ) such that  $O_{|\uparrow\rangle} = g_\alpha O_{|\downarrow\rangle}$  and  $O_{|\uparrow\rangle} = g_\alpha O_{|\downarrow\rangle}$ . In this way, we ensure that there is a symmetry operation connecting the opposite sublattices  $O_{|\uparrow\rangle}$  and  $O_{|\downarrow\rangle}$ . Therefore, the magnetic configurations described by  $O_{|\uparrow\rangle}$  and  $O_{|\downarrow\rangle}$  may have collinear antiferromagnetism or altermagnetism.

To further determine whether the magnetic configurations described by  $O_{|\uparrow\rangle}$  and  $O_{|\downarrow\rangle}$  possess altermagnetism, it is necessary to analyze the symmetry between the sublattices. In three-dimensional materials, when there are symmetry operations between the opposite sublattices whose point group parts are included  $\{E, \bar{E}\}$ , or in two-dimensional materials, when these elements are included in  $\{E, \bar{E}, C_{2z}, m_z\}$ , it results in  $\varepsilon(\vec{s}, \vec{k}) = \varepsilon(-\vec{s}, \vec{k})$ , leading to spin degeneracy [1]. Consequently, if opposite sublattices in three-dimensional materials possess symmetry operations that encompass  $\{E, \tau\} \otimes_S \{E, \bar{E}\}$  or, in two-dimensional materials,  $\{E, \tau\} \otimes_S \{E, \bar{E}, C_{2z}, m_z\}$ , where  $\tau$  represents any translation operation, this leads to spin degeneracy. Therefore, the opposite sublattices of altermagnetic orders cannot be linked by the aforementioned symmetry operations.

For example, when  $f_1 = C_2$ , where  $C_2$  is a twofold rotation operation around an axis in the  $xy$  plane, the group  $G$  can be decomposed into  $G = H \cup C_2 H$ , and its orbits can be decomposed into  $\{hx \mid h \in H\}$  and  $\{gx \mid g \in C_2 H\}$ . When up spins occupy the orbit  $\{hx \mid h \in H\}$  and down spins occupy  $\{gx \mid g \in C_2 H\}$ , or vice versa, there is always  $O_{|\downarrow\rangle} = C_2 O_{|\uparrow\rangle}$ . Additionally,  $O_{|\uparrow\rangle}$  may not be transformed into  $O_{|\downarrow\rangle}$  through any symmetry operation belonging to the set  $\{E, \tau\} \otimes_S \{E, \bar{E}\}$  (and for two-dimensional magnetic materials, this also encompasses the set  $\{E, \tau\} \otimes_S \{E, \bar{E}, C_{2z}, m_z\}$ ). Therefore, collinear magnetic configuration may possess altermagnetism. If from  $O_{|\uparrow\rangle}$  one is able to obtain  $O_{|\downarrow\rangle}$  through such symmetry operations, the magnetic configuration possesses antiferromagnetism.

This general approach can generate collinear magnetic configurations, including those with antiferromagnetism and altermagnetism. After obtaining the possible collinear magnetic configurations, we consider the symmetry between the opposite sublattices to determine whether each magnetic configuration possesses altermagnetism. We retain multicomponent candidate structures obtained in Sec. II that may have



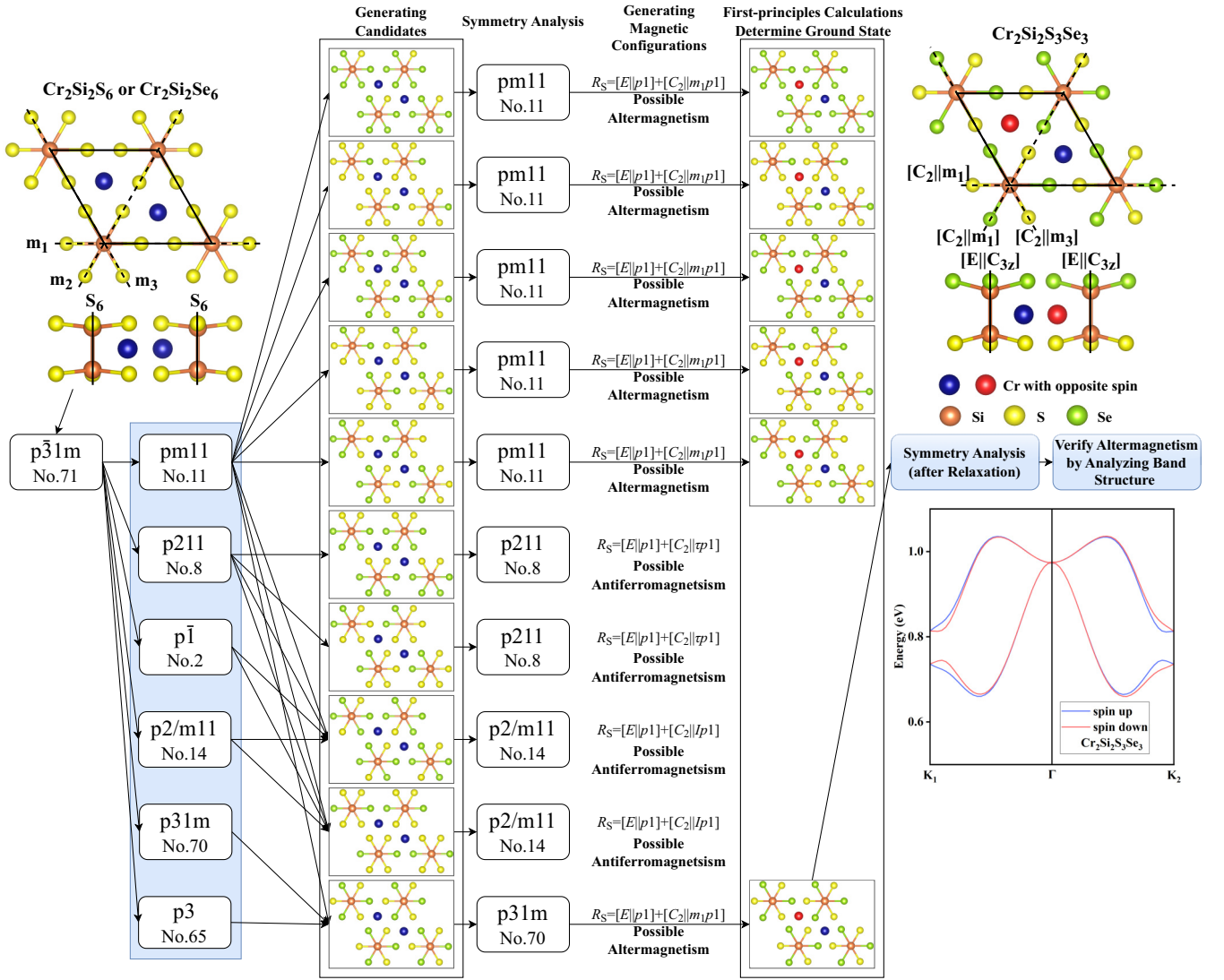


FIG. 3. An example of searching for altermagnetic structures in the multicomponent structure compound  $\text{Cr}_2\text{Si}_2\text{S}_{6x}\text{Se}_{6(1-x)}$ . Blue and red balls represent Cr atoms, with different colors of atoms representing opposite spin sublattices, respectively. Yellow balls represent S atoms, green balls represent Se atoms, or vice versa. Orange balls represent Si atoms.

altermagnetic configurations among all possible collinear magnetic configurations. Then for each candidate we use first-principles calculations to determine the energy of different magnetic configurations, and identify its magnetic ground state. By combining symmetry analysis and first-principles calculations, we have discovered several materials with two-dimensional altermagnetism, as presented in Sec. IV, and the structural files are detailed in Supplemental Material [26].

#### IV. PRACTICAL EXAMPLES FOR TWO-DIMENSIONAL MULTICOMPONENT ALTERMAGNETS

In a two-dimensional material database (such as C2DB), classifying materials by layer groups can yield a set of materials with the same symmetry. In such materials, a batch of magnetic materials with similar chemical formulas and structures can be screened out, such as  $A_2B_2C_6$  ( $\text{Mn}_2\text{P}_2\text{S}_6$ ,  $\text{Mn}_2\text{P}_2\text{Se}_6$ ,  $\text{Cr}_2\text{Si}_2\text{S}_6$ ,  $\text{Li}_2\text{Mn}_2\text{Cl}_6$ ). Materials such as  $\text{Cr}_2\text{Si}_2\text{S}_6$  and  $\text{Cr}_2\text{Si}_2\text{Se}_6$  possess similar symmetries, corresponding to

the space group  $p\bar{3}1m$  (layer group No. 71). In these materials, sulfur (S) and selenium (Se) atoms are in equivalent positions. Taking  $\text{Cr}_2\text{Si}_2\text{S}_{6x}\text{Se}_{6(1-x)}$  as an example, we generate multicomponent structures with altermagnetism. These structures are derived from the primitive cell, with magnetic configurations obtained using supercells up to four times the size of the primitive cell. Given that  $a_1$  and  $a_2$  are the primitive translation vectors of the primitive cell, and  $c_1$  and  $c_2$  are those of the supercell, the latter can be expressed in terms of the former through an integer transformation matrix  $P$ ,  $\begin{pmatrix} c_1 \\ c_2 \end{pmatrix} = P \begin{pmatrix} a_1 \\ a_2 \end{pmatrix} = \begin{pmatrix} P_{11} & P_{12} \\ P_{21} & P_{22} \end{pmatrix} \begin{pmatrix} a_1 \\ a_2 \end{pmatrix}$ . Materials  $\text{Cr}_2\text{Si}_2\text{S}_6$  and  $\text{Cr}_2\text{Si}_2\text{Se}_6$  have symmetry corresponding to  $p\bar{3}1m$  (layer group No. 71). We analyze all the subgroups of the layer group  $p\bar{3}1m$ . The layer group  $p\bar{3}1m$  has nontrivial subgroups  $p\bar{1}$ ,  $pm11$ ,  $cm11$ ,  $p211$ ,  $c211$ ,  $c2m11$ ,  $p3$ ,  $p\bar{3}$ ,  $p312$ ,  $p31m$ . Corresponding to different subgroups  $H_k$ , the equivalent positions in the primitive cell are divided into different subgroup  $H_k$  orbits. After obtaining the orbits, we populate these orbits with elements and generate a

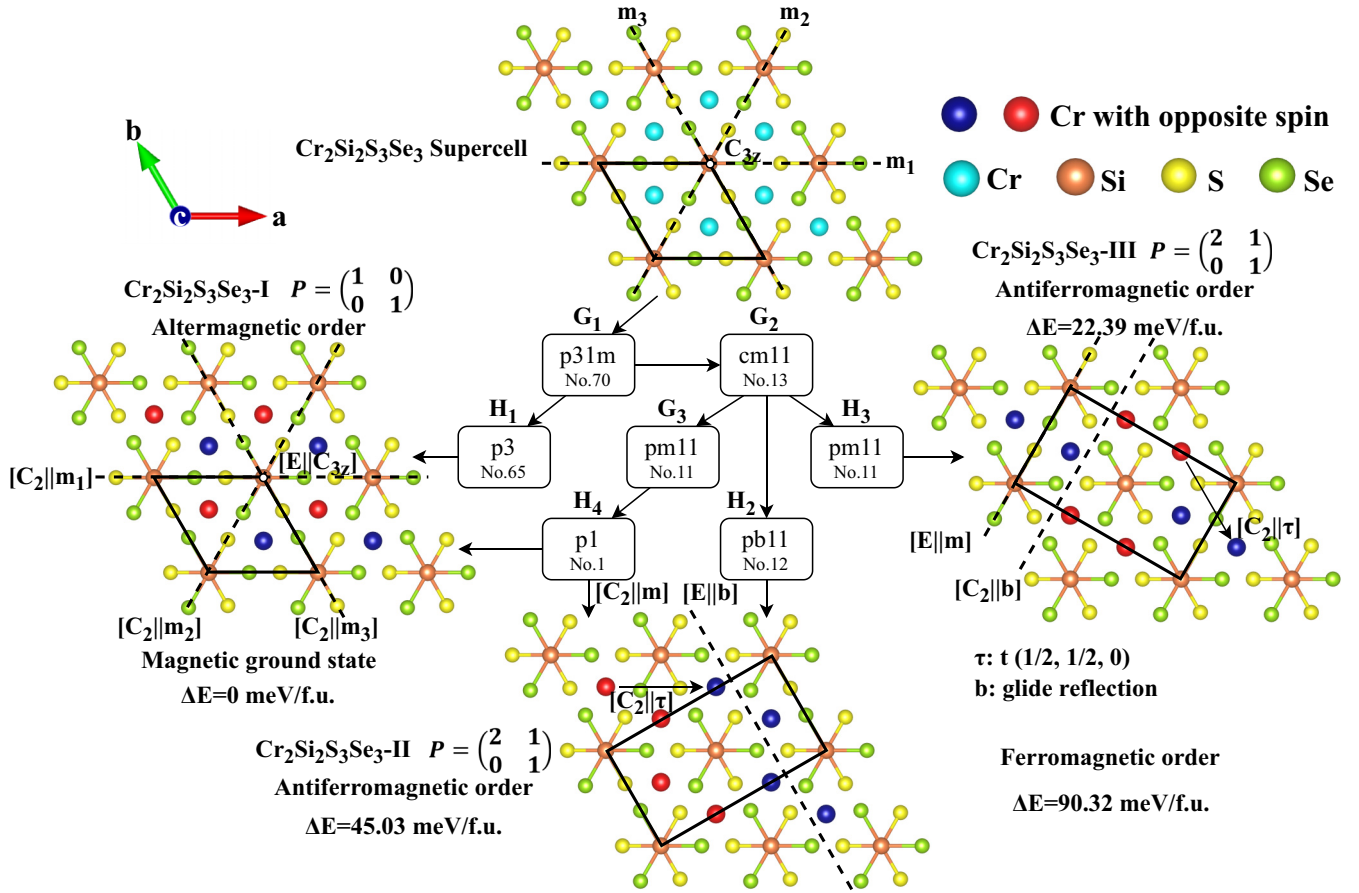


FIG. 4. An example of generating opposite-spin sublattices in  $\text{Cr}_2\text{Si}_2\text{S}_3\text{Se}_3$ , which are connected by symmetry operations, is demonstrated based on the methods introduced in Sec. III. Cyan, blue, and red balls represent Cr atoms, with red and blue balls representing opposite spin sublattices, respectively. Yellow balls represent S atoms, green balls represent Se atoms, and light purple balls represent P atoms.  $\Delta E$  denotes the excess energy per formula unit compared to the magnetic ground state. The notation/f.u. represents averaging to each formula unit.

series of candidates with specific symmetries  $H_k$ . During this process, equivalent structures may be generated, which need to be deduplicated. After eliminating equivalent structures, there are only 12 candidates, some of which are shown in Fig. 3. If the supercell is considered, more candidates may be obtained. Based on the methods introduced in Sec. III, we generate collinear magnetic configurations for  $\text{Cr}_2\text{Si}_2\text{S}_3\text{Se}_3$ . By analyzing the symmetry operations that connect the opposite sublattices, we determine whether these structures can possess altermagnetism. Then, we retain candidate structures that may have altermagnetism, narrowing down our selection to six candidates, which are shown in Fig. 3. After that, we use first-principles calculations to determine the magnetic ground state of these candidates, thereby judging whether they indeed possess altermagnetism. The ionic relaxation step in DFT calculations may alter the symmetry of the structures, hence a new symmetry analysis is required after the ionic relaxation.

To systematically explore altermagnetism in multicomponent systems, we focus on  $\text{Cr}_2\text{Si}_2\text{S}_3\text{Se}_3$  (as shown in Fig. 4), which was selected from the six candidate  $\text{Cr}_2\text{Si}_2\text{S}_{6x}\text{Se}_{6(1-x)}$  structures with potential altermagnetism and serves as a representative example. Utilizing the method introduced in Sec. III for generating collinear magnetic configurations, we generated collinear magnetic configurations for

the candidate material  $\text{Cr}_2\text{Si}_2\text{S}_3\text{Se}_3$  using supercells up to four times the size of the primitive cell. These supercells are defined by distinct integer transformation matrices  $P = \begin{pmatrix} 2 & 1 \\ 0 & 1 \end{pmatrix}, \begin{pmatrix} 2 & 1 \\ -1 & 1 \end{pmatrix}, \begin{pmatrix} 3 & 1 \\ 0 & 1 \end{pmatrix}, \begin{pmatrix} 2 & 0 \\ 1 & 2 \end{pmatrix}, \begin{pmatrix} 2 & 0 \\ 0 & 2 \end{pmatrix}$ . Employing first-principles calculations, we evaluated the energies of diverse magnetic configurations for the candidate structure  $\text{Cr}_2\text{Si}_2\text{S}_3\text{Se}_3$  and subsequently identified the magnetic ground state. The energies of different collinear magnetic configurations are shown in Figs. 4 and 5.

The candidate  $\text{Cr}_2\text{Si}_2\text{S}_3\text{Se}_3$  has the symmetry of group  $G_1$ , corresponding to  $p31m$  (layer group No. 70). The group  $G_1$  is generated by the set of generators  $\langle \tau(1, 0, 0), \tau(0, 1, 0), C_{3z}, m^{(1)} \rangle$  and can be decomposed into cosets of half group  $H_1$  ( $p3$ , layer group No. 65), which is generated by the set of generators  $\langle \tau(1, 0, 0), \tau(0, 1, 0), C_{3z} \rangle$ . The  $G_1$  orbit of position  $x$  occupied by a Cr atom can be decomposed into  $\{hx | h \in H_1\}$  and  $\{gx | g \in m^{(1)}H_1\}$ . When up spins occupy  $\{hx | h \in H_1\}$  and down spins occupy  $\{gx | g \in m^{(1)}H_1\}$ , or vice versa, both cases result in  $O_{|\downarrow} = m^{(1)}O_{|\uparrow}$ . By iterating through the orbital occupation patterns, we obtain one magnetic configuration denoted as  $\text{Cr}_2\text{Si}_2\text{S}_3\text{Se}_3$ -I, shown in Fig. 4.

Group  $G_1$  has a  $t$  subgroup  $G_2$ , corresponding to  $cm11$  (layer group No. 13), which is generated by the set

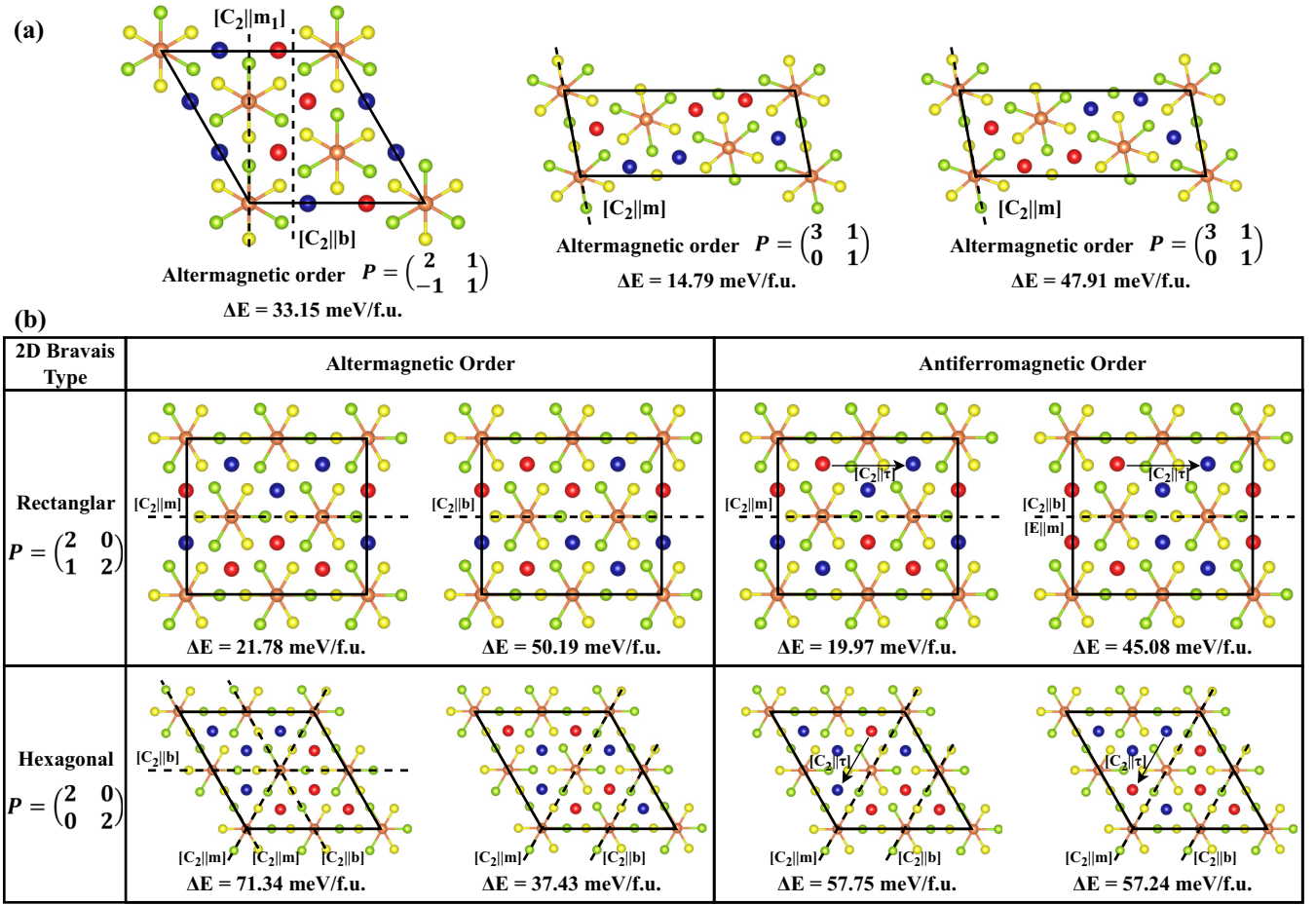


FIG. 5. Utilizing the methods introduced in Sec. III, a greater number of collinear magnetic configurations can be obtained by larger supercells that are three (a) and four (b) times the size of the primitive cell of  $\text{Cr}_2\text{Si}_2\text{S}_3\text{Se}_3$ . By selecting supercells of different 2D Bravais types, a wider variety of collinear magnetic configurations can be generated. Cyan, blue, and red balls represent Cr atoms, with red and blue balls representing opposite spin sublattices, respectively. Yellow balls represent S atoms, green balls represent Se atoms, and light purple balls represent P atoms.  $\Delta E$  denotes the excess energy per formula unit compared to the magnetic ground state. The notation /f.u. represents averaging to each formula unit.

of generators  $\langle \tau(1, 0, 0), \tau(1, 0, 0), \tau(\frac{1}{2}, \frac{1}{2}, 0), m \rangle$ , where  $m$  is the mirror operation in the  $yz$  plane. Subgroup  $H_2$  (which corresponds to  $pb11$ , layer group No. 12) is generated by the set of generators  $\langle \tau(1, 0, 0), \tau(1, 0, 0), b \rangle$ , where  $b = \tau(\frac{1}{2}, \frac{1}{2}, 0)m$ . Because the set of generators  $\langle \tau(1, 0, 0), \tau(1, 0, 0), \tau(\frac{1}{2}, \frac{1}{2}, 0), m \rangle$  of  $G_2$  can be expressed as  $\langle \tau(1, 0, 0), \tau(1, 0, 0), m, b \rangle$ ,  $G_2$  can be decomposed into cosets of the half group  $H_2$ . Employing a two-times larger cell, the  $G_2$  orbit of position  $x$  occupied by a Cr atom can be decomposed into  $\{hx \mid h \in H_2\}$  and  $\{gx \mid g \in mH_2\}$ . When up spins occupy  $\{hx \mid h \in H_2\}$  and down spins occupy  $\{gx \mid g \in mH_2\}$ , or vice versa, both cases result in  $O_{|\downarrow\rangle} = mO_{|\uparrow\rangle}$ . By iterating through the orbital occupation patterns, we obtain another magnetic configuration denoted as  $\text{Cr}_2\text{Si}_2\text{S}_3\text{Se}_3\text{-II}$ , as shown in Fig. 4.

In addition, subgroup  $H_3$  (which corresponds to  $pm11$ , layer group No. 11) is generated by the set of generators  $\langle \tau(1, 0, 0), \tau(1, 0, 0), m \rangle$ . Therefore,  $G_2$  can be decomposed into cosets of the half group  $H_3$ . Employing a two-times larger cell, the  $G_2$  orbit of position  $x$  occupied by a Cr atom can be decomposed into  $\{hx \mid h \in H_3\}$  and  $\{gx \mid g \in \tau(\frac{1}{2}, \frac{1}{2}, 0)H_3\}$ .

When up spins occupy  $\{hx \mid h \in H_3\}$  and down spins occupy  $\{gx \mid g \in \tau(\frac{1}{2}, \frac{1}{2}, 0)H_3\}$ , or vice versa, both cases result in  $O_{|\downarrow\rangle} = \tau(\frac{1}{2}, \frac{1}{2}, 0)O_{|\uparrow\rangle}$ . By iterating through the orbital occupation patterns, we obtain another magnetic configuration denoted as  $\text{Cr}_2\text{Si}_2\text{S}_3\text{Se}_3\text{-III}$ , shown in Fig. 4.

Based on the analysis of the candidates  $\text{Cr}_2\text{Si}_2\text{S}_3\text{Se}_3$ , the sublattice  $O_{|\uparrow\rangle}$  occupied by up spins in the magnetic configuration  $\text{Cr}_2\text{Si}_2\text{S}_3\text{Se}_3\text{-I}$  cannot obtain the opposite sublattice  $O_{|\downarrow\rangle}$  through inversion operation  $\bar{E}$ , translation operation  $\tau$ , rotation operation  $C_{2z}$  around an axis parallel to the  $z$  axis, mirror operation  $m_z$  parallel to the  $xy$  plane, or their products with translation operation  $\tau$ . Therefore, the magnetic configuration  $\text{Cr}_2\text{Si}_2\text{S}_3\text{Se}_3\text{-I}$  meets the symmetry requirement of altermagnetism. In the cases of  $\text{Cr}_2\text{Si}_2\text{S}_3\text{Se}_3\text{-II}$  and  $\text{Cr}_2\text{Si}_2\text{S}_3\text{Se}_3\text{-III}$ , the sublattice  $O_{|\uparrow\rangle}$  occupied by up spins can obtain the opposite sublattice  $O_{|\downarrow\rangle}$  through performing a translation symmetry operation  $\tau(\frac{1}{2}, \frac{1}{2}, 0)$ . Hence, the magnetic configurations  $\text{Cr}_2\text{Si}_2\text{S}_3\text{Se}_3\text{-II}$  and  $\text{Cr}_2\text{Si}_2\text{S}_3\text{Se}_3\text{-III}$  possess antiferromagnetism.

Based on the three-times and four-times larger supercells, we obtain a greater variety of collinear magnetic



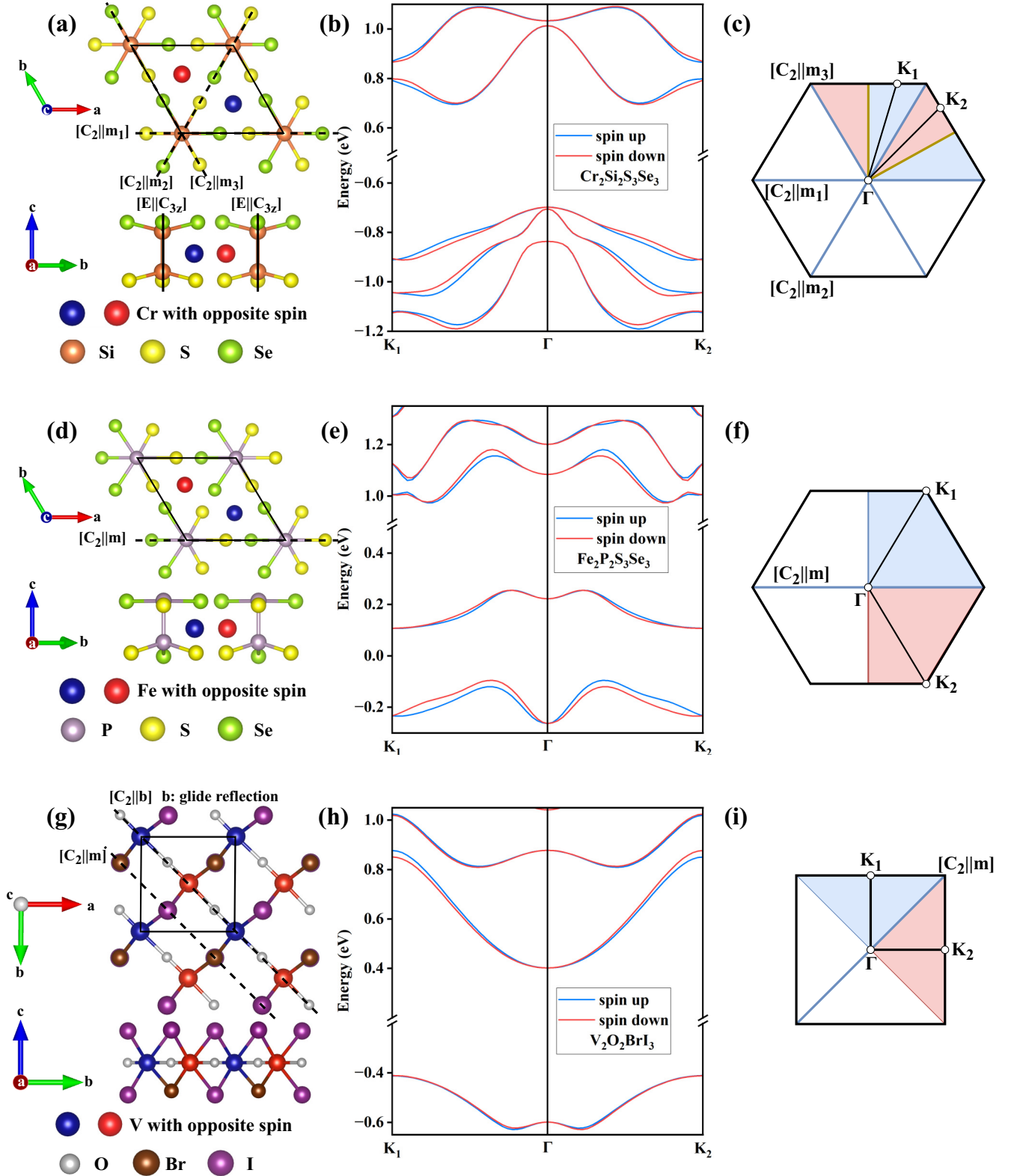


FIG. 6. The crystal structures and nonrelativistic band structures of  $\text{Cr}_2\text{Si}_2\text{S}_3\text{Se}_3$ ,  $\text{Fe}_2\text{P}_2\text{S}_3\text{Se}_3$ , and  $\text{V}_2\text{O}_2\text{BrI}_3$ . The crystal structures of  $\text{Cr}_2\text{Si}_2\text{S}_3\text{Se}_3$  (a),  $\text{Fe}_2\text{P}_2\text{S}_3\text{Se}_3$  (d), and  $\text{V}_2\text{O}_2\text{BrI}_3$  (g), where different colors represent the opposite spin sublattices. The band structures of  $\text{Cr}_2\text{Si}_2\text{S}_3\text{Se}_3$  (b),  $\text{Fe}_2\text{P}_2\text{S}_3\text{Se}_3$  (e), and  $\text{V}_2\text{O}_2\text{BrI}_3$  (h) without SOC along the  $\mathbf{k}$  path  $K_1$ - $\Gamma$ - $K_2$  show spin splitting, where blue and red solid line represent the opposite spin channels. The  $\mathbf{k}$  path we use to calculate the band structures of  $\text{Cr}_2\text{Si}_2\text{S}_3\text{Se}_3$  (c),  $\text{Fe}_2\text{P}_2\text{S}_3\text{Se}_3$  (f), and  $\text{V}_2\text{O}_2\text{BrI}_3$  (i). The different colors represent opposite spins.



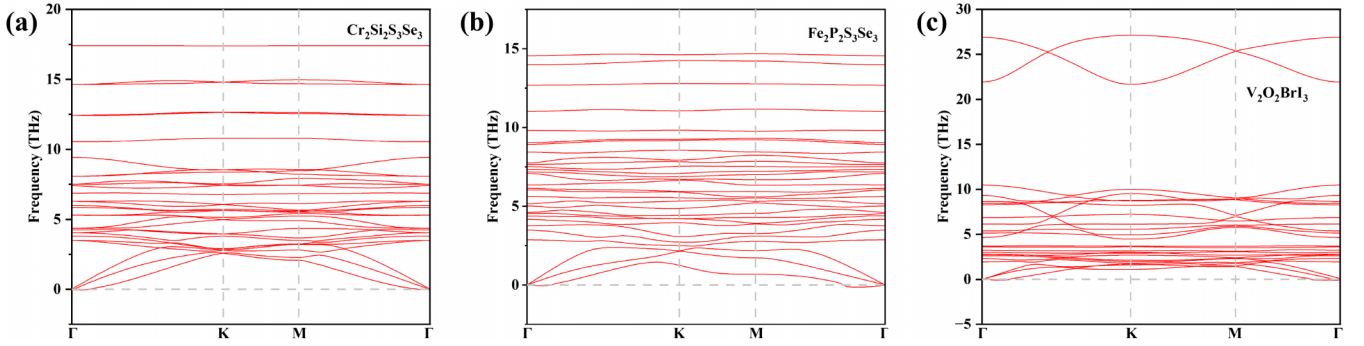


FIG. 7. Phonon-dispersion spectrum for  $\text{Cr}_2\text{Si}_2\text{S}_3\text{Se}_3$  (a),  $\text{Fe}_2\text{P}_2\text{S}_3\text{Se}_3$  (b), and  $\text{V}_2\text{O}_2\text{BrI}_3$  (c).

configurations. In particular, by choosing supercells of different 2D Bravais types, we can produce a more diverse range of collinear magnetic configurations. Through the aforementioned methods, we generated a series of collinear magnetic configurations with opposite sublattices connected by symmetry operations. After eliminating magnetic configurations that are equivalent, we are left with 12 unique configurations, as shown in Fig. 5. First-principles calculations confirm that the altermagnetic configuration  $\text{Cr}_2\text{Si}_2\text{S}_3\text{Se}_3$ -I is the magnetic ground state, with an energy per formula unit lower than other magnetic configurations, and 90.32 meV lower compared to the ferromagnetic configuration. To confirm the altermagnetism of  $\text{Cr}_2\text{Si}_2\text{S}_3\text{Se}_3$ , we conducted first-principles calculations to analyze nonrelativistic band structure [shown in Fig. 6(b)], focusing on the crystal-momentum ( $\mathbf{k}$ ) dependent spin splitting. Therefore, we obtain the structure  $\text{Cr}_2\text{Si}_2\text{S}_3\text{Se}_3$  with two-dimensional altermagnetism. Utilizing a similar approach, we generate two-dimensional material  $\text{Fe}_2\text{P}_2\text{S}_3\text{Se}_3$  with altermagnetism. The crystal structure and nonrelativistic band structure of  $\text{Fe}_2\text{P}_2\text{S}_3\text{Se}_3$  are shown in Figs. 6(d) and 6(e).

In addition to  $\text{Cr}_2\text{Si}_2\text{S}_3\text{Se}_3$  and  $\text{Fe}_2\text{P}_2\text{S}_3\text{Se}_3$  having hexagonal lattices, we generate two-dimensional material  $\text{V}_2\text{O}_2\text{Br}_{4x}\text{I}_{4(1-x)}$  having altermagnetism with a rectangular lattice, based on the same method. The symmetry of two-dimensional magnetic materials  $\text{VOBr}_2$  and  $\text{VOI}_2$  corresponds to layer group  $pm2m$  (No. 27). The  $pm2m$  layer group has subgroups  $p11m$ ,  $p211$ , and  $pm11$ . For each distinct subgroups  $H_k$ , the positions of Br and I atoms within the supercell defined by  $P = \begin{pmatrix} 1 & 1 \\ -1 & 1 \end{pmatrix}$  are partitioned into  $H_k$  orbits. We allow components to occupy all atomic positions on the orbits and generate candidate structures with specific symmetries  $H_k$ . After removing equivalent structures, we obtain seven candidates. We generate possible magnetic configurations of candidates  $\text{V}_2\text{O}_2\text{Br}_{4x}\text{I}_{4(1-x)}$ . In order to determine whether these structures can possess altermagnetism, we analyze the symmetry operations that connect the opposite sublattices. Then, candidates  $\text{V}_2\text{O}_2\text{BrI}_3$ ,  $\text{V}_2\text{O}_2\text{BrI}_2$ , and  $\text{V}_2\text{O}_2\text{BrI}$ , which may possess altermagnetism, are retained for first-principles calculations. Through first-principles calculations and the band structure analysis, it was determined that the magnetic ground states of the candidates  $\text{V}_2\text{O}_2\text{BrI}_3$  [shown in Fig. 6(g)],  $\text{V}_2\text{O}_2\text{BrI}_2$ , and  $\text{V}_2\text{O}_2\text{BrI}$  are altermagnetic. The magnetic ground state of the candidate  $\text{V}_2\text{O}_2\text{BrI}_3$  has an energy per formula unit 13.24 meV lower than that of the ferromagnetic order; the magnetic ground state of

the candidate  $\text{V}_2\text{O}_2\text{BrI}_2$  has an energy per formula unit 28.67 meV lower; and the magnetic ground state of the candidate  $\text{V}_2\text{O}_2\text{BrI}$  has an energy per formula unit 31.04 meV lower.

## V. SUMMARY

In summary, we have provided a general approach to generating multicomponent structures with two-dimensional altermagnetism, as well as a systematic method for generating collinear magnetic configurations where opposite-spin lattices are interconnected through symmetry operations. While this study primarily focuses on the application of generating candidate structures with specific symmetries and collinear magnetic configurations in two-dimensional altermagnets, the proposed methodology is equally applicable to three-dimensional systems. We anticipate that this approach will significantly contribute to the discovery of novel altermagnetic materials in future research. Meanwhile, we identified several stable two-dimensional altermagnetic materials, validating the use of this approach in the search for 2D altermagnets. Furthermore, this approach generates a rich variety of collinear magnetic configurations that meet symmetry requirements, improving the accuracy of magnetic ground state predictions. Among the series of altermagnetic materials, we have provided structures with dynamic stability, providing a reference for the experimental synthesis of two-dimensional altermagnetic materials.

## ACKNOWLEDGMENTS

This work is supported by the Guangdong Basic and Applied Basic Research Foundation (Grants No. 2023A1515110894 and No. 2023A1515012289) and by the National Natural Science Foundation of China (Grants No. 12074126 and No. 12474228). This work is partially supported by High Performance Computing Platform of South China University of Technology.

## DATA AVAILABILITY

The data that support the findings of this article are openly available in the Supplemental Material [26].

## APPENDIX A: COMPUTATIONAL DETAILS

All calculations were performed using the Vienna *Ab initio* Simulation Package (VASP) [27,28], employing the projector

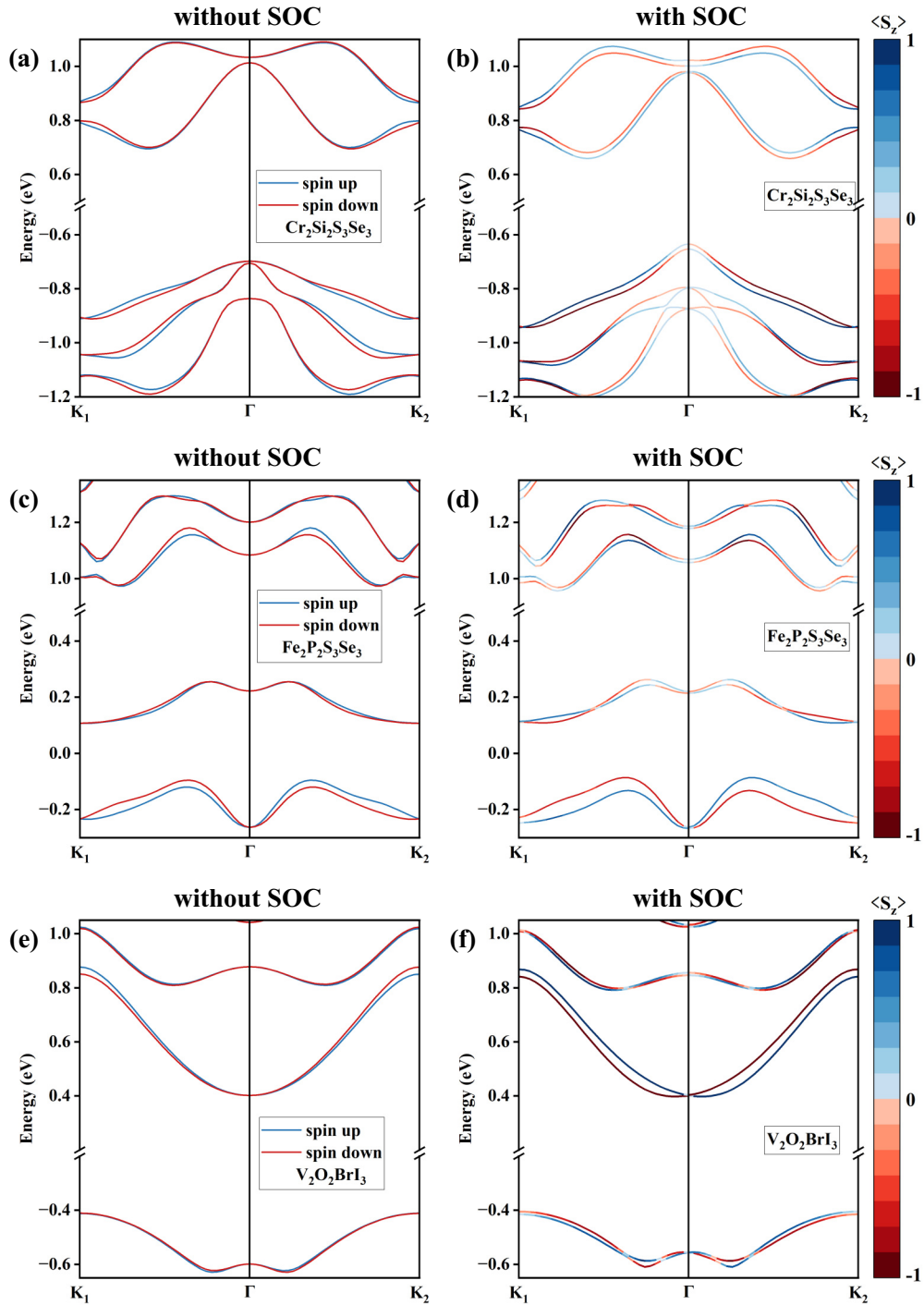


FIG. 8. The band structures for  $\text{Cr}_2\text{Si}_2\text{S}_3\text{Se}_3$  (a),  $\text{Fe}_2\text{P}_2\text{S}_3\text{Se}_3$  (c), and  $\text{V}_2\text{O}_2\text{BrI}_3$  (e) are presented without SOC, while their counterparts with SOC are shown in (b), (d), and (f), respectively.

augmented wave method [29] based on density functional theory. A cutoff energy of 500 eV was set for the plane wave basis. The structure was relaxed until the forces on atoms were below 0.001 eV/Å, and the convergence criterion was  $1 \times 10^{-7}$  eV for the energy difference in the electronic self-consistent calculation. A vacuum of 12 Å was applied perpendicular to the material plane. The SOC effect was not considered in the calculations.

## APPENDIX B: DYNAMIC STABILITY

To evaluate the dynamic stability, we calculated the phonon spectrum of the two-dimensional altermagnetic structures  $\text{Cr}_2\text{Si}_2\text{S}_3\text{Se}_3$ ,  $\text{Fe}_2\text{P}_2\text{S}_3\text{Se}_3$ , and  $\text{V}_2\text{O}_2\text{BrI}_3$ , as shown in Fig. 7. The absence of any negative phonon frequencies confirms the dynamical stability of the structures  $\text{Cr}_2\text{Si}_2\text{S}_3\text{Se}_3$ ,  $\text{Fe}_2\text{P}_2\text{S}_3\text{Se}_3$ , and  $\text{V}_2\text{O}_2\text{BrI}_3$  in our predictions.

TABLE I. List of multicomponent altermagnets. We state the layer groups (LG), spin layer groups (SLG) without SOC, magnetic layer groups (MLG) with SOC, and the easy axis.

	LG	SLG w/o SOC	MLG w SOC	Easy axis
$\text{Cr}_2\text{Si}_2\text{S}_3\text{Se}_3$	$p31m$	$p^13^11^{-1}m$	$pm'11$	$\hat{x}$
$\text{Fe}_2\text{P}_2\text{S}_3\text{Se}_3$	$pm11$	$p^{-1}m^11^11$	$pm11$	$\hat{y}$
$\text{V}_2\text{O}_2\text{BrI}_3$	$cm11$	$c^{-1}m^11^11$	$cm11$	$\hat{y}$

## APPENDIX C: BAND STRUCTURE WITH SOC

In this Appendix we provide a comparison of band structures with and without SOC for all materials, as illustrated in Fig. 8. Our results show that SOC effects do not suppress the altermagnetic spin-splitting phenomenon. Upon incorporating SOC effects, the symmetry of the candidate structures reduces from the spin layer group to the magnetic layer group. The easy axis of magnetization and magnetic layer groups of the candidate structures were analyzed, as listed in Table I.

- [1] I. Mazin, Altermagnetism then and now, *Physics* **17**, 4 (2024).
- [2] L. Šmejkal, J. Sinova, and T. Jungwirth, Emerging research landscape of altermagnetism, *Phys. Rev. X* **12**, 040501 (2022).
- [3] L. Šmejkal, J. Sinova, and T. Jungwirth, Beyond conventional ferromagnetism and antiferromagnetism: A phase with nonrelativistic spin and crystal rotation symmetry, *Phys. Rev. X* **12**, 031042 (2022).
- [4] L. Bai, W. Feng, S. Liu, L. Šmejkal, Y. Mokrousov, and Y. Yao, Altermagnetism: Exploring new frontiers in magnetism and spintronics, *Adv. Funct. Mater.* **34**, 2409327 (2024).
- [5] I. Mazin (The PRX Editors), Editorial: Altermagnetism—A new punch line of fundamental magnetism, *Phys. Rev. X* **12**, 040002 (2022).
- [6] I. I. Mazin, Altermagnetism in MnTe: Origin, predicted manifestations, and routes to detwinning, *Phys. Rev. B* **107**, L100418 (2023).
- [7] T. A. Maier and S. Okamoto, Weak-coupling theory of neutron scattering as a probe of altermagnetism, *Phys. Rev. B* **108**, L100402 (2023).
- [8] Z. Feng, X. Zhou, L. Šmejkal, L. Wu, Z. Zhu, H. Guo, R. González-Hernández, X. Wang, H. Yan, P. Qin *et al.*, An anomalous Hall effect in altermagnetic ruthenium dioxide, *Nat. Electron.* **5**, 735 (2022).
- [9] M. Naka, S. Hayami, H. Kusunose, Y. Yanagi, Y. Motome, and H. Seo, Spin current generation in organic antiferromagnets, *Nat. Commun.* **10**, 4305 (2019).
- [10] A. Bose, N. J. Schreiber, R. Jain, D.-F. Shao, H. P. Nair, J. Sun, X. S. Zhang, D. A. Muller, E. Y. Tsybal, D. G. Schlom *et al.*, Tilted spin current generated by the collinear antiferromagnet ruthenium dioxide, *Nat. Electron.* **5**, 267 (2022).
- [11] K.-H. Ahn, A. Hariki, K.-W. Lee, and J. Kuneš, Antiferromagnetism in  $\text{RuO}_2$  as  $d$ -wave Pomeranchuk instability, *Phys. Rev. B* **99**, 184432 (2019).
- [12] S. Lee, S. Lee, S. Jung, J. Jung, D. Kim, Y. Lee, B. Seok, J. Kim, B. G. Park, L. Šmejkal, C.-J. Kang, and C. Kim, Broken Kramers degeneracy in altermagnetic MnTe, *Phys. Rev. Lett.* **132**, 036702 (2024).
- [13] H.-Y. Ma, M. Hu, N. Li, J. Liu, W. Yao, J.-F. Jia, and J. Liu, Multifunctional antiferromagnetic materials with giant piezomagnetism and noncollinear spin current, *Nat. Commun.* **12**, 2846 (2021).
- [14] F. Zhang, X. Cheng, Z. Yin, C. Liu, L. Deng, Y. Qiao, Z. Shi, S. Zhang, J. Lin, Z. Liu, M. Ye, Y. Huang, X. Meng, C. Zhang, T. Okuda, K. Shimada, S. Cui, Y. Zhao, G.-H. Cao, S. Qiao, J. Liu, and C. Chen, Crystal-symmetry-paired spin-valley locking in a layered room-temperature metallic altermagnet candidate, *Nat. Phys.* (2025).
- [15] B. Jiang, M. Hu, J. Bai, Z. Song, C. Mu, G. Qu, W. Li, W. Zhu, H. Pi, Z. Wei, Y.-J. Sun, Y. Huang, X. Zheng, Y. Peng, L. He, S. Li, J. Luo, Z. Li, G. Chen, H. Li, H. Weng, and T. Qian, A metallic room-temperature  $d$ -wave altermagnet, *Nat. Phys.* (2025).
- [16] L. Šmejkal, A. B. Hellenes, R. González-Hernández, J. Sinova, and T. Jungwirth, Giant and tunneling magnetoresistance in unconventional collinear antiferromagnets with nonrelativistic spin-momentum coupling, *Phys. Rev. X* **12**, 011028 (2022).
- [17] S. Reimers, L. Odenbreit, L. Šmejkal, V. N. Strocov, P. Constantinou, A. B. Hellenes, R. J. Ubierno, W. H. Campos, V. K. Bharadwaj, A. Chakraborty *et al.*, Direct observation of altermagnetic band splitting in CrSb thin films, *Nat. Commun.* **15**, 2116 (2024).
- [18] S. Zeng and Y.-J. Zhao, Description of two-dimensional altermagnetism: Categorization using spin group theory, *Phys. Rev. B* **110**, 054406 (2024).
- [19] J. Sodequist and T. Olsen, Two-dimensional altermagnets from high throughput computational screening: Symmetry requirements, chiral magnons, and spin-orbit effects, *Appl. Phys. Lett.* **124**, 182409 (2024).
- [20] I. Mazin, R. González-Hernández, and L. Šmejkal, Induced monolayer altermagnetism in  $\text{MnP}(\text{S,Se})_3$  and  $\text{FeSe}$ , *arXiv:2309.02355*.
- [21] S. Zeng and Y.-J. Zhao, Bilayer stacking A-type altermagnet: A general approach to generating two-dimensional altermagnetism, *Phys. Rev. B* **110**, 174410 (2024).
- [22] B. Pan, P. Zhou, P. Lyu, H. Xiao, X. Yang, and L. Sun, General stacking theory for altermagnetism in bilayer systems, *Phys. Rev. Lett.* **133**, 166701 (2024).
- [23] S. Hastrup, M. Strange, M. Pandey, T. Deilmann, P. S. Schmidt, N. F. Hinsche, M. N. Gjerding, D. Torelli, P. M. Larsen, A. C. Riis-Jensen, J. Gath, K. W. Jacobsen, J. Jørgen Mortensen, T. Olsen, and K. S. Thygesen, The Computational 2D Materials Database: high-throughput modeling and discovery of atomically thin crystals, *2D Mater.* **5**, 042002 (2018).
- [24] M. N. Gjerding, A. Taghizadeh, A. Rasmussen, S. Ali, F. Bertoldo, T. Deilmann, N. R. Knøsgaard, M. Kruse, A. H. Larsen, S. Manti, T. G. Pedersen, U. Petralanda, T. Skovhus, M. K. Svendsen, J. J. Mortensen, T. Olsen, and K. S. Thygesen, Recent progress of the computational 2D materials database (C2DB), *2D Mater.* **8**, 044002 (2021).

- [25] Y.-J. Cen, C.-C. He, S.-B. Qiu, Y.-J. Zhao, and X.-B. Yang, Determining ground states of alloys by a symmetry-based classification, *Phys. Rev. Mater.* **6**, L050801 (2022).
- [26] See Supplemental Material at <http://link.aps.org/supplemental/10.1103/PhysRevB.111.195123> for additional information about all the structures with altermagnetism proposed in this paper.
- [27] G. Kresse and J. Furthmüller, Efficiency of *ab-initio* total energy calculations for metals and semiconductors using a plane-wave basis set, *Comput. Mater. Sci.* **6**, 15 (1996).
- [28] G. Kresse and J. Furthmüller, Efficient iterative schemes for *ab initio* total-energy calculations using a plane-wave basis set, *Phys. Rev. B* **54**, 11169 (1996).
- [29] G. Kresse and D. Joubert, From ultrasoft pseudopotentials to the projector augmented-wave method, *Phys. Rev. B* **59**, 1758 (1999).